# Two-Dimensional and Three-Dimensional Analyses of Sigma Precipitates and Porosity in a Superaustenitic Stainless Steel

R.W. FONDA, E.M. LAURIDSEN, W. LUDWIG, P. TAFFOREAU, and G. SPANOS

X-ray micro-tomography revealed not only the true three-dimensional (3-D) distribution, interconnectivity, and morphology of coarse sigma precipitates in an AL-6XN superaustenitic stainless steel, but also the presence of an internal void network associated with these precipitates. The voids were present within the bulk of the undeformed material, indicating that they formed during alloy fabrication. The presence of these voids in association with the brittle sigma particles has important implications for the mechanical behavior of these alloys.

## I. INTRODUCTION

THE alloy AL-6XN is often referred to as a "superaustenitic" stainless steel due to both its composition and its properties. Conventional austenitic stainless steels exhibit an excellent combination of high strength, toughness, ductility, and formability. In addition, those steels typically exhibit a corrosion resistance superior to that of martensitic or ferritic steels, and can retain their excellent strength and corrosion resistance at elevated temperatures. AL-6XN has a similar (20 to 22 wt pct) chromium content to other austenitic stainless steels, but differs from those steels with a high content (~24 wt pct) of nickel and a significant amount (~6 wt pct) of molybdenum[1] (Table I). These compositional changes provide a better resistance to corrosion (particularly pitting corrosion, crevice corrosion, and stress corrosion cracking), an improved yield strength, and a higher elevated temperature strength than exhibited by the 300 series stainless steels, while maintaining good ductility and toughness.[1,2]

As is well known, during casting (including the continuous casting process typically used during fabrication of AL-6XN), alloying elements segregate into the interdendritic regions. Because solidification proceeds from the plate surface to the center, rejection of solute into the interdendritic regions results in an increasing solute concentration in the interdendritic regions toward the center of the plate. Subsequent hot rolling flattens and elongates these solute-enriched regions into compositional bands. When these bands contain sufficient levels of chromium and molybdenum, they are suscep-

tible to the formation of the sigma phase.[3,4] Thus, the maximum susceptibility to sigma formation is usually observed near the plate centerline.

It has been shown that the presence of sigma precipitates can be quite detrimental to the mechanical properties of alloys. In particular, sigma is a hard and brittle phase, and is therefore notorious for reducing toughness.[3–6] Brittle particles such as sigma may fracture during deformation, potentially initiating cracks or widening into interparticle voids during continued deformation. Sigma precipitation also removes chromium and molybdenum from the austenite matrix, reducing the corrosion resistance of the alloy.[1,7] The initial purpose of the current research was to use both conventional two-dimensional (2-D) microscopy techniques and three-dimensional (3-D) X-ray microtomography to determine the distribution and connectivity of sigma along the centerline of a continuously cast and hot-rolled plate of AL-6XN. As will be shown subsequently, the 3-D analysis revealed some unexpected distributions of voids that have important implications on the properties of this material.

Previous studies[8–12] have shown that the presence of hard particles within a material can lead to void formation during hot working. Hard particles will not distort uniformly with the softer matrix during deformation. Instead, the deformation generates flow incompatibilities at the matrix-particle interface, with the matrix flowing around the hard particle. If the matrix loses contact with the particle, the matrix-particle interface fails and a crack is generated. The deformation required to achieve this interfacial debonding varies with many factors, including the type of deformation, the difference in mechanical properties between the particle and the matrix, the interfacial bond strength between the particle and the matrix, the location of the particle within the material, and the size and shape of the particle. For the case of rolling deformation, large particles near the plate surface or centerline are the most likely to experience this interfacial debonding due to the larger material flow gradients at those locations. This debonding can result in the formation of conical voids at

| Fe | Ni | Cr | Mo | Mn | Cu | C | Si | N | P | S |
|---|---|---|---|---|---|---|---|---|---|---|
| bal. | 24.0 | 20.5 | 6.2 | 0.40 | 0.2 | 0.02 | 0.40 | 0.22 | 0.020 | 0.001 |

**Table I. Composition of the AL-6XN Plate, in Weight Percent[1]**

the ends of the particle, aligned with the direction of material flow.[8–10]

The flow incompatibilities that lead to void formation increase with the size of the particle. There is therefore a threshold size, called the critical inclusion size, above which particles are likely to generate voids during hot working. This critical inclusion size also varies with the deformation process and material parameters, but has been determined by Klevebring and co-workers[11,12] to be approximately 2.5 to 3.5 $\mu$m for silica particles and 4 to 7.5 $\mu$m for (Fe,Mn)O inclusions in hot-worked steel.

The presence of voids within a material, whether they are generated by brittle fracture of particles or as a result of interfacial debonding around the particles, can have a deleterious effect on the mechanical properties of that material. Because stress cannot be transmitted across the void itself, the load is transferred instead to the adjacent material. The resultant stress concentration facilitates local yielding at the void, reducing the strength of the material.[13]

## II. EXPERIMENTAL

A specimen of AL-6XN known to contain some centerline sigma precipitation was used in this study. This material was continuously cast, hot cross rolled to the finishing width, and then hot rolled in a single direction down to a final plate thickness of 6.35 mm (0.25 in.) and annealed at about 950 °C. Cross sections of the as-received plate were polished and then etched with a modified oxalic acid etch[1] to reveal the morphology and distribution of the sigma phase, as viewed on a 2-D plane of polish, by optical microscopy. In this procedure, a solution of 100 g oxalic acid in 900 mL water was used to etch the surface for 3 to 5 seconds at an applied potential of 6 V. Scanning electron microscopy was also performed on polished cross-sectional surfaces using the backscattered electron signal.

Specimens for X-ray tomography were machined along the centerline from selected regions containing appropriate distributions of sigma precipitation. The machined samples had a geometry consisting of a base 3-mm tall and 3 mm in diameter, which supported a post that was 2-mm tall and initially 500 $\mu$m in diameter. All tomography observations were made on the post portion of the sample. The initial X-ray tomography scans were performed on samples of this geometry. The post of one sample was thinned further with 1000-grit paper to a final diameter of approximately 150 $\mu$m. The tomography reconstructions presented here are from this smaller diameter specimen, although the characteristics reported from that sample were also observed in the larger diameter specimens. An energy of 20.5 keV, which is slightly above the Mo

absorption edge, was selected to enhance the absorption contrast of the sigma precipitates in the tomographic scans. Tomography was conducted at the micro-tomography beamline (ID19) at the European Synchrotron Radiation Facility (Grenoble, France) using a setup providing a spatial resolution of approximately 1.4 $\mu$m.

## III. RESULTS AND DISCUSSION

Near the centerline of the plate, both compositional banding and sigma precipitation are often observed (Figure 1(a)). The compositional banding is most pronounced along the centerline and can vary from a single moderate band to the multiple strong bands shown in Figure 1(a). Sigma precipitates can form within these solute-enriched bands and will vary in size and distribution depending on the magnitude of the compositional segregation. Thus, even though this particular specimen contained significant sigma, nearly half of the total centerline length was devoid of sigma precipitation. In regions where sigma was observed, it was usually only present within one or occasionally two of the compositional bands. The typical number of compositional bands containing sigma is therefore significantly less than that shown in Figure 1. The region shown in Figure 1 was selected to highlight the variations that can
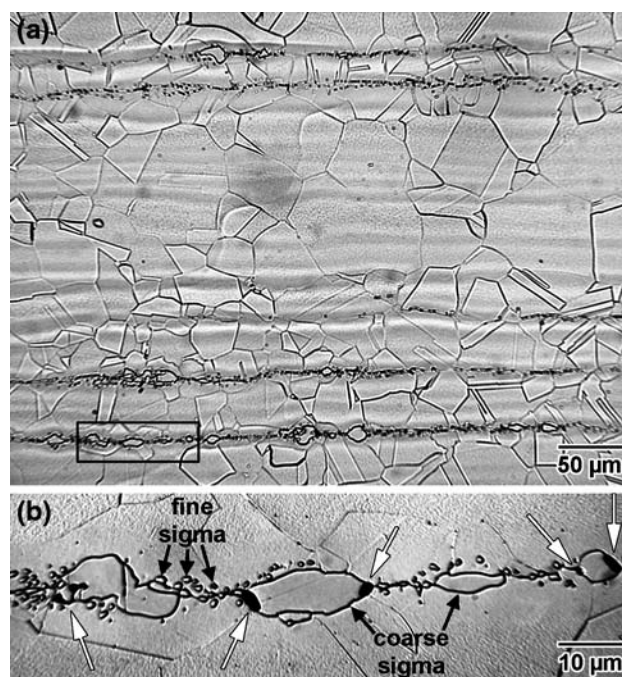


Fig. 1—Optical micrograph of AL-6XN, showing (a) compositional bands and the associated sigma precipitation, and (b) enlargement from the indicated region in (a) displaying sigma precipitate sizes and distributions. White arrows indicate voids.

be observed in compositional band strength and spacing, as well as in sigma precipitate distributions.

Sigma precipitation within these bands of compositional segregation appears to occur with two distinct size ranges and morphologies (Figure 1(b)). Wherever sigma is observed, there are fine sigma precipitates that are only a few microns in size. These fine precipitates often appear to be equiaxed when viewed on 2-D planes of polish, although more elongated 2-D shapes are not uncommon (Figure 1(b)). Many of these regions also contain much coarser sigma particles, usually about 10 to 20 $\mu$m in size. These coarse precipitates are observed in the larger and more strongly segregated compositional bands and have 2-D morphologies ranging from equiaxed to very complex and irregular.

The morphology of the sigma precipitates and their distribution within the austenitic matrix is more clearly demonstrated, at least in 2-D, by scanning electron microscopy and crystal orientation maps (Figure 2). The coarse sigma precipitates have an irregular distribution, but tend to be associated with high concentrations of the fine sigma precipitates. This is not unexpected, because the banded regions with very high solute concentrations should result in increased precipitation of sigma in general, regardless of size or shape. Grain growth is inhibited by the distribution of sigma precipitates along the centerline, contributing to an observed finer grain size along the centerline, as compared to other locations across the plate cross section (Figure 2(c)).

Chemical analysis reveals that the sigma particles are strongly enriched in molybdenum (Figure 3). This enrichment was beneficial in imaging the sigma phase during the X-ray tomography experiments. Specifically, because molybdenum has an absorption edge at 20.0 KeV, an X-ray energy of 20.5 keV was selected during the tomography scans to enhance the contrast due to this molybdenum segregation. The sigma also exhibits a slight enrichment in chromium and depletions in both iron and nickel (Figure 3).

X-ray tomography revealed the true 3-D distribution and size of the coarse sigma particles along the plate centerline. The fine sigma precipitates were not observed by this technique, as they were below the resolution of the detector. The distribution and size of the coarse sigma on each 2-D tomography slice (light regions in Figure 4) were similar to those obtained by the conventional 2-D optical and electron microscopy techniques discussed previously (compare Figure 4 to Figures 1 through 3). Three-dimensional reconstruction of these data (Figure 5) reveals that the sigma precipitates lie on a nearly planar band. Individual sigma precipitates range in size from about 5 to 15 $\mu$m and usually exhibit a near-equiaxed morphology. However, many sigma precipitates instead form adjacent to other precipitates, creating the appearance of larger precipitates with a more irregular shape, as was often observed by the 2-D techniques.

The tomography scans also revealed the presence of internal voids in association with the coarse sigma precipitates. These voids appear as dark regions in Figure 4. Full 3-D reconstruction of the voids from the tomography data (Figure 5(a)) reveals that these voids
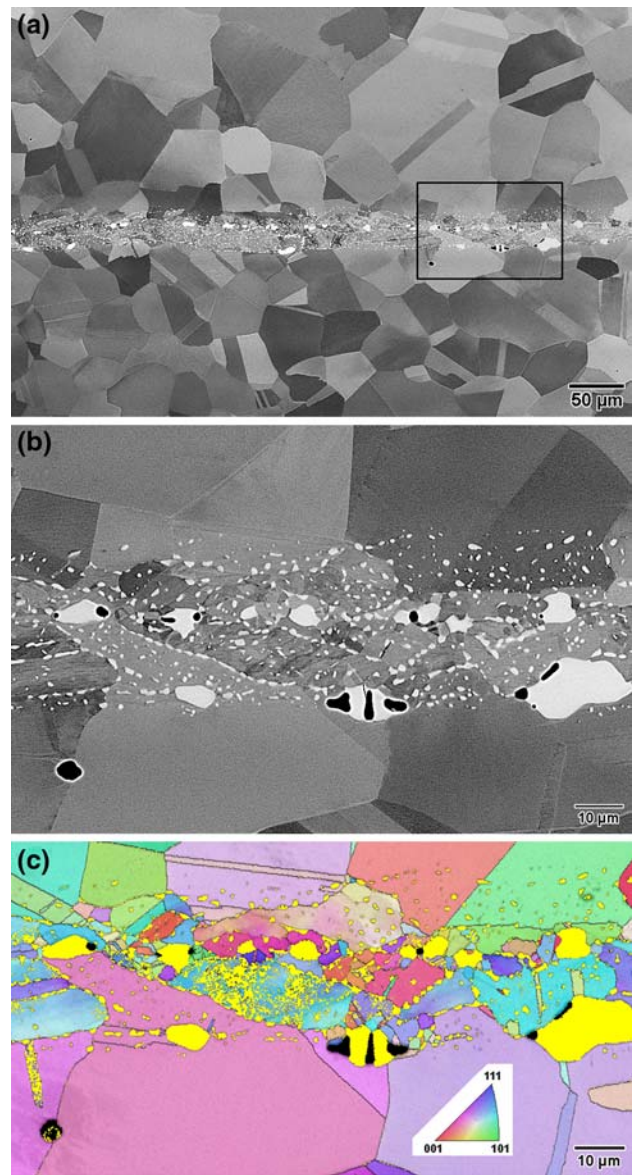


Fig. 2—(a) Scanning electron micrograph (backscattered electron image) of the centerline sigma within the austenite matrix, (b) enlargement from the indicated region in (a) showing details of the sigma precipitation, and (c) electron backscattered diffraction results from the same area showing sigma (yellow) within the austenite matrix (colors indicate austenite crystal orientation (inset)).

exist both as isolated voids and as more extensive void networks. When the tomography data from both the voids and the coarse sigma precipitates are visualized together (Figures 5(b) and (c)), it becomes evident that the voids are localized in a nearly planar region near the center of the band of coarse sigma particles. In addition, there is a definite correlation between the voids and the coarse sigma particles. Both the isolated voids and the void networks are invariably associated with specific coarse sigma particles, and almost every coarse sigma particle is associated with at least one void. While some voids are associated with only a single coarse sigma particle, most voids form between two or more adjacent coarse sigma particles. Such voids either form a
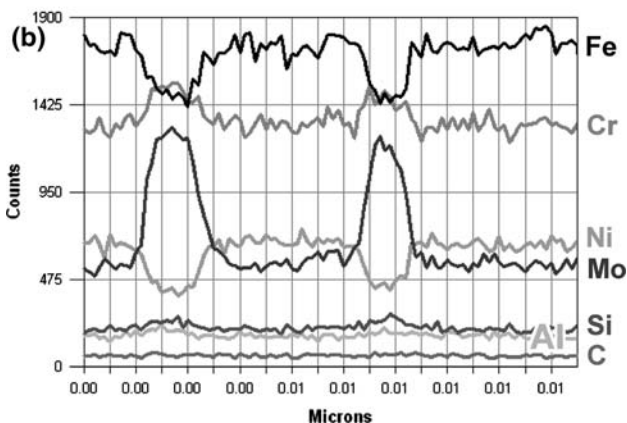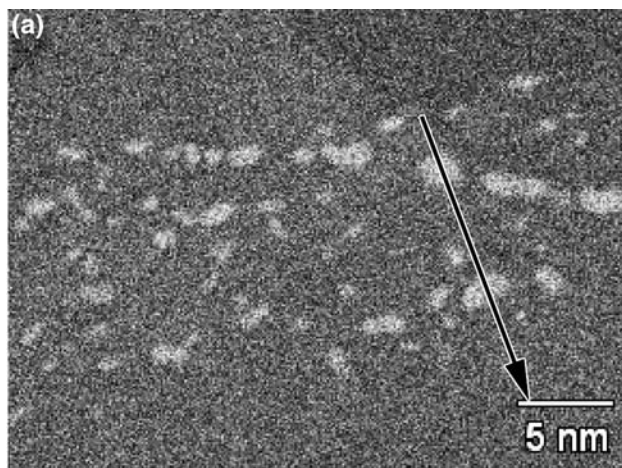
Fig. 3—(a) Backscattered scanning electron micrograph of sigma precipitation and (b) energy-dispersive X-ray analysis of composition along the indicated line.
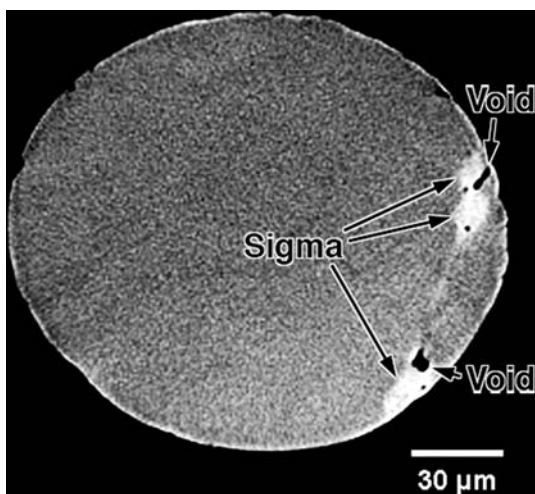


Fig. 4—One slice from the X-ray tomography data showing voids associated with the coarse sigma particles in 2-D.

boundary between adjacent particles or possess the morphology of an elongated link connecting nearby particles (Figure 5(b)).

The internal voids observed by the 3-D X-ray tomography technique can, in retrospect, also be seen

in the 2-D sections examined by optical microscopy (Figure 1) and scanning electron microscopy (Figure 2). These voids were observed in all samples containing the coarse sigma, but have not been reported by previous researchers. The likely explanation for this is that, because all previous studies of centerline sigma precipitation had been conducted on the 2-D surface of mechanically polished specimens, fracture and pullout of a brittle precipitate phase such as sigma were not unexpected. It was thus often assumed in these earlier studies that these voids were polishing artifacts. However, the current 3-D tomographic analysis on the interior of an undeformed, bulk sample demonstrates that these voids are actually present in the interior of the material, and are therefore not produced during sample preparation.

The voids observed in this study appear to arise from two sources. Most voids are located at one or both ends of a coarse sigma particle, aligned with the final rolling direction of the plate. The locations and shapes of these voids suggest that they were formed during a planar deformation process (i.e., rolling). Furthermore, because the voids are generally aligned with the final rolling direction, they likely formed during the final rolling stages and not during the initial casting or cross-rolling of the plate. These voids at the ends of the particles often resemble the voids predicted for planar or hot-rolling deformation,[8–10] wherein flow incompatibilities between the hard particles and the matrix produce an interfacial debonding that evolves during further deformation into conical-shaped voids at the ends of the particles. Some voids, such as the vertical void near the center of Figures 2(b) and (c), are located between two sigma particles. Such voids often exhibit similar, or even planar, boundaries with the two sigma particles. These voids thus appear to have formed through fracture of the sigma and subsequent opening of that crack during further deformation.

The voids were always observed to be associated with coarse sigma particles that were more than 5 $\mu$m in size. While the smaller (2 to 3 $\mu$m) sigma precipitates, and presumably any voids that would have formed in association with them, were below the resolution of this tomography experiment, extensive optical microscopy and scanning electron microscopy did not reveal any voids in association with those small precipitates. This is consistent with the critical inclusion sizes determined by Klevebring and co-workers.[11,12] They observed that silica particles above 2.5 to 3.5 $\mu$m or (Fe,Mn)O inclusions above 4 to 7.5 $\mu$m were required to form voids during hot working of steel. This indicates that, in order to prevent void formation along the centerline during rolling, it is only necessary to avoid formation of the coarse sigma particles, because the very fine sigma particles appear to be smaller than the critical void nucleation size.

The revelation of such ubiquitous internal void networks associated with the coarse sigma particles along the centerline of the AL-6XN plate has important implications. First, even though a feature may have the characteristics of an expected specimen preparation artifact, that feature does not necessarily arise from
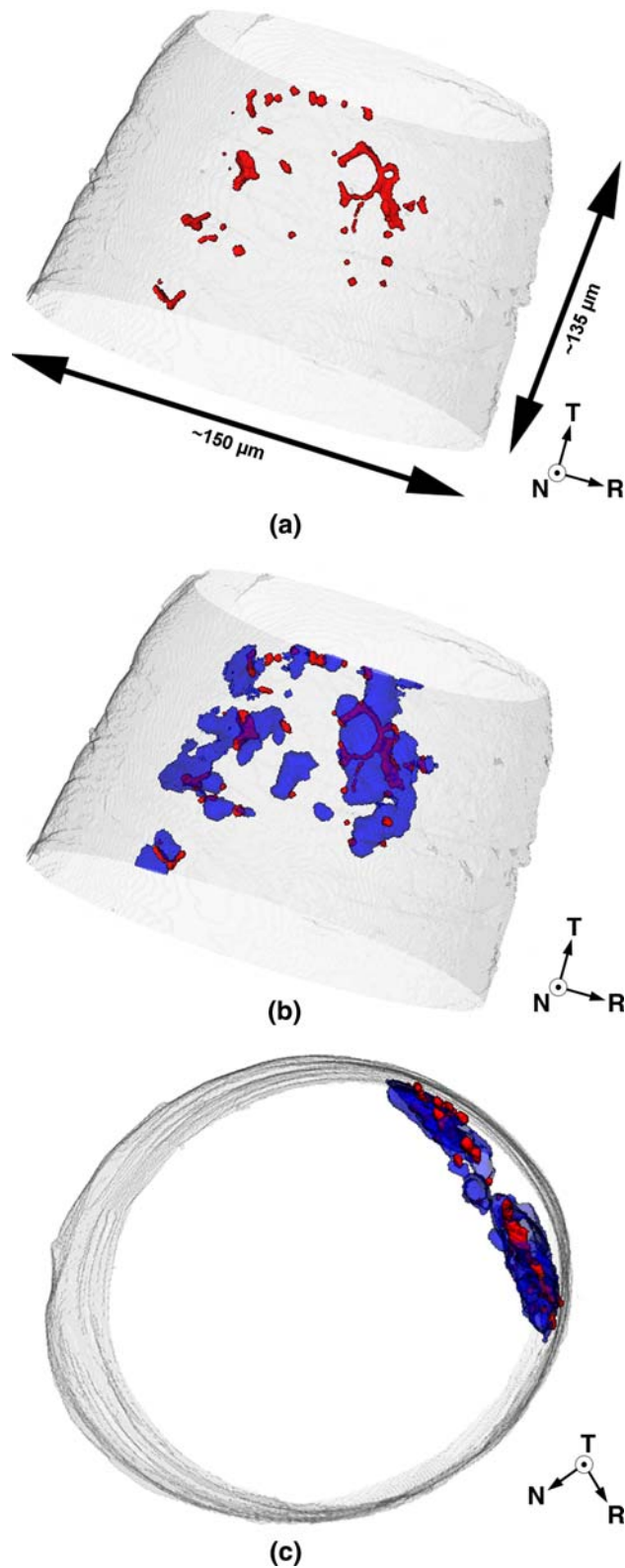
Fig. 5—3-D X-ray tomography reconstructions showing (*a*) the isolated voids and void networks on the centerline plane, (*b*) the spatial association between the voids (red) and sigma precipitates (blue), and (*c*) the distribution of voids and sigma precipitates as viewed along the centerline plane. Directions shown indicate the thickness or plate normal direction (*N*), the final rolling direction (*R*), and the transverse direction (*T*).

the specimen preparation process. This article demonstrates that pores associated with the brittle sigma phase on a polished surface generally corresponded to voids that were produced during plate fabrication and were not a result of pullout during specimen preparation. The presence of brittle sigma precipitates along the centerline has long been known to be detrimental to the mechanical properties of such plate geometries.[3,5,6] However, the current results indicate that the voids may be at least as significant as (or even more significant than) the sigma precipitates in affecting the final mechanical properties. Furthermore, this research suggests that sigma precipitation may have a less direct role in reducing toughness than was previously thought. The decrease in toughness may be more a function of the voids formed in association with the sigma particles during hot rolling than from the brittle nature of the sigma particles themselves. The presence of voids in association with the brittle sigma precipitates can therefore have a severe effect on crack initiation and growth in these alloys. In particular, the anomalous longitudinal cracking along the centerline observed by Stauffer *et al.*[4] can be readily explained by a pre-existing network of voids along the centerline. Specific tests to determine the relative influences of the coarse sigma precipitates and the void networks on the mechanical behavior of this steel were not performed due to the close association between these two features and their very nonuniform distribution across even short distances in this alloy. This research further emphasizes the importance of developing processing schemes to avoid the formation of the coarse sigma precipitates and their associated void networks, as well as the benefits of 3-D microstructural analyses to properly correlate the features in such networks.

## IV. SUMMARY

Micro-tomography of the sigma phase along the centerline of an Al-6XN superaustenitic steel plate revealed not only the true 3-D distribution, interconnectivity, and morphology of coarse sigma particles, but also the presence of internal void networks associated with and lying in the same plane as the coarse sigma particles. One rather startling finding of the X-ray tomography observations was that almost every coarse sigma particle was associated with at least one void. While some voids were associated with a single coarse sigma particle, the voids were often observed between two or more adjacent coarse sigma particles, either as a boundary between the particles or linking those particles across a short distance. Most voids appear to result from flow incompatibilities between the matrix and particle during deformation, although other voids appear to be the product of particle fracture and opening of that crack during further deformation. These centerline void-plus-sigma particle networks can severely impact the mechanical properties of the plate, and their observation re-emphasizes the importance of proper processing schemes to minimize the formation

of the coarse sigma precipitates and their associated void networks. The fact that these void networks had not been reported in AL-6XN based on previous conventional 2-D microscopy observations demonstrates that (1) features that appear to be specimen preparation artifacts may in fact be very important features of the microstructure that can significantly alter the material properties, and (2) 3-D microstructural characterization techniques are essential to elucidate these types of complex networked microstructural features.

## REFERENCES

1. *AL-6XN Alloy*, 3rd ed., Allegheny Ludlum, Pittsburgh, PA, 2005.
2. S. Nemat-Nasser, W.-G. Guo, and D.P. Kihl: *J. Mech. Phys. Solids*, 2001, vol. 49, pp. 1823–46.
3. C.J. Novak: in *Handbook of Stainless Steels*, D. Peckner, ed., McGraw-Hill, New York, NY, 1977, pp. 4-1–4-78.
4. A.C. Stauffer, D.A. Koss, and J.B. McKirgan: *Metall. Mater. Trans. A*, 2004, vol. 35A, pp. 1317–24.
5. E.C. Bain and W.E. Griffiths: *Trans. AIME*, 1927, vol. 75, pp. 166–213.
6. A.M. Talbot and D.E. Furman: *Trans. ASM*, 1953, vol. 45, pp. 429–42.
7. M. Schwind, J. Källqvist, J.-O. Nilsson, J. Ågren, and H.-O. Andrén: *Acta Mater*, 2000, vol. 48, pp. 2473–81.
8. S. Rudnik: *J. Iron Steel Inst.*, 1966, vol. 204, pp. 374–76.
9. C. Luo: *Comp. Mater. Sci.*, 2001, vol. 21, pp. 360–74.
10. E. Ervasti and U. Ståhlberg: *J. Mater. Proc. Technol.*, 2005, vol. 170, pp. 142–50.
11. B.-I. Klevebring, E. Bogren, and R. Mahrs: *Metall. Trans. A*, 1975, vol. 6A, pp. 319–27.
12. B.-I. Klevebring: *Scand. J. Metall.*, 1976, vol. 5, pp. 63–68.
13. A.S. Tetelman and A.J. McEvily, Jr.: *Fracture of Structural Materials*, John Wiley & Sons, Inc, New York, NY, 1967, pp. 14–34.